Non-Covalent Interactions between Unsolvated Peptides: Helical Complexes Based on Acid−Base Interactions

Rajagopalan Sudha, Motoya Kohtani, and Martin F. Jarrold*

Chemistry Department, Indiana University, 800 East Kirkwood Avenue, Bloomington, Indiana 47405-7102

Received: October 4, 2004

We have used ion-mobility mass spectrometry to examine the conformations of the protonated complex formed between AcA_7KA_6KK and $AcEA_7EA_7$, helical alanine-based peptides that incorporate glutamic acid (E) and lysine (K). Designed interactions between the acidic E and basic K residues help to stabilize the complex, which is generated by electrospray and studied in the gas phase. There are two main conformations: (1) a coaxial linear arrangement where the helices are tethered together by an EKK interaction between the pair of lysines at the C-terminus of the AcA_7KA_6KK peptide and a glutamic acid at the N-terminus of the $AcEA_7EA_7$ peptide and (2) a coiled-coil arrangement with side-by-side antiparallel helices where there is an additional EK interaction between the E and K residues in the middle of the helices. The coiled-coil opens up to the coaxial linear structure as the temperature is raised. Entropy and enthalpy changes for the opening of the coiled-coil were derived from the measurements. The enthalpy change indicates that the interaction between the E and K residues in the middle of the helices is a weak neutral hydrogen bond. The EKK interaction is significantly stronger.

Introduction

Noncovalent interactions play an important role in the structure and function of biomolecules. One of the most common noncovalent interactions in proteins is the hydrogen bond between acidic residues (glutamic acid or aspartic acid) and basic residues (arginine or lysine). These interactions play an important role in protein folding and stability.[1−8] In aqueous solution, glutamic acid (E) and lysine (K) positioned at i,i+4 in an α-helix can form a hydrogen-bonded ion pair (resulting from proton transfer from E to K). This type of interaction has been used to stabilize α-helices and coiled-coils.[9−14] In the gas phase, ion-pair formation is less favorable, and in the absence of other stabilizing factors (such as a charge or dipole), E and K are expected to interact through a neutral hydrogen bond. In the study reported here, we have used interactions between E and K to help stabilize complexes between two helical alanine-based peptides (AcA_7KA_6KK and $AcEA_7EA_7$).

The aggregation of secondary structural elements into domains provides model systems to understand the tertiary and quaternary structural motifs in proteins. Studies of unsolvated peptides and proteins provide insight into the intramolecular interactions that are important in protein folding[15−22] and helps to unravel the complex interplay between intramolecular interactions and solution interactions. Electrospray is known to be soft enough to maintain noncovalent interactions,[23−26] and peptide aggregates are frequently observed in electrospray mass spectra.[27−29] In the work reported here, we use ion-mobility mass spectrometry to examine the conformations of a peptide complex generated by electrospray. The mobility of an ion depends on its average collision cross section, which in turn depends on its conformation. Ions with open structures undergo more collisions with the buffer gas and travel more slowly than ions with compact structures.[30−32] To assign the geometries, average collision cross sections are obtained from the mobility measurements and compared to the cross sections calculated for trial structures derived from molecular dynamics simulations.

The ion mobility method has been successfully used to determine the conformations of unsolvated peptide ions[33−36] and peptide complexes.[37−39] For example, trimers produced by electrospraying a mixture of $Ac(GA)_7K$ and $AcA(GA)_7K$ appear to have a pinwheel geometry consisting of three helices tethered together by an exchanged lysine motif, where the protonated lysine side chains associate with the C-termini of neighboring helices. Mixtures of helix-forming peptides Ac-A_{14}K and Ac-A_{15}K, and Ac-$(GA)_7$K and Ac-$A(GA)_7$K have been shown to yield V-shaped complexes where the helices are tethered together by an exchanged lysine interaction. The globule-forming peptides Ac-$K(GA)_7$ and Ac-$KA(GA)_7$ form mainly globular complexes. However, an antiparallel coiled-coil arrangement of helices is a minor component for the Ac-$K(GA)_7$·Ac-$KA(GA)_7+2H^+$ complex. The coiled-coil is dominant for the Ac-KA_{14}·Ac-$KA_{15}+2H^+$ complex.[38] In these last two examples, the coiled-coil arrangement allows favorable charge-dipole interactions that are not possible in the isolated peptides.

Design of Peptides

In the present study, we examine complexes of helical peptides that are stabilized by interactions between acidic and basic residues. Alanine has a high helix propensity in the gas phase. Unsolvated alanine-based peptides form stable α-helices when there is a positive charge near the C-terminus[29,33,40] because a charge in that location interacts favorably with the helix dipole. A negative charge near the N-terminus is also expected to be helix stabilizing. Hence, K residues are placed near the C-terminus in the AcA_7KA_6KK peptide, and an E residue is placed at the N terminus in $AcEA_7EA_7$. The other K and E residues are located at i+7/i+8 positions so that their side chains are on the same faces of the α-helices. A double lysine (KK) is placed at the C-terminus of the K peptide. As

* To whom correspondence should be addressed. E-mail: mfj@indiana.edu.

10.1021/jp045490m CCC: $30.25
Published on Web 03/10/2005

we discuss further below, the interaction of a KK with an E is expected to be stronger than a single EK interaction. In addition to the EKK interaction expected at the termini of the helices, the peptides are designed to have an EK interaction in the middle. The E and K peptides are designed to be complementary so that they associate to form an antiparallel coiled-coil. This arrangement is also stabilized by favorable interactions between the helix dipoles.

Materials and Methods

The peptides were synthesized using FastMoc chemistry on an Applied Biosystems 433A peptide synthesizer. After synthesis, they were cleaved from the HMP resin using a 95% TFA and 5% water v/v mixture, precipitated using cold diethyl ether and lyophilized. The peptides were used without further purification. Equimolar mixtures of the E and K peptides (0.5 mM) were dissolved in a mixture of 1 mL TFA and 0.1 mL water and electrosprayed. The doubly charged complex was mass selected, and mobility measurements were performed. The peptides are not expected to form complexes in the TFA solutions used in this study, and so the complexes are most likely formed during the electrospray process.

Mobility measurements were performed using a home-built ion mobility mass spectrometer which is described fully in a previous paper.[41] Electrosprayed peptide ions enter a differentially pumped region through a heated capillary interface held at 380−400 K. After passing through this region, the ions are focused into the drift tube. The drift tube is 30.5 cm long and filled with 2.5−4.0 mbar of helium. The drift tube temperature was varied between 173 and 563 K in these studies. Two different drift tubes were used to cover this temperature range: one optimized for temperatures below 400 K and the other optimized for temperatures above 300 K. The drift voltage was 280 V. After the ions exit the drift tube, they are passed through a quadrupole mass spectrometer and are then detected with a collision dynode and two stacked microchannel plates. The time taken by the ions to travel across the drift tube (the drift time) is determined using an electrostatic shutter to permit 100-μs packets of ions to enter the drift tube and recording their arrival time distribution at the detector using a multichannel scaler that is synchronized with the electrostatic shutter. The drift time is proportional to the average collision cross section.[42] Peaks in the drift-time distributions are assigned by comparing their collision cross sections to average collision cross sections calculated for conformations derived from molecular dynamics (MD) simulations.

The MD simulations were performed using the MACSIMUS suite of programs[43] with the CHARMM 21.3 parameter set. Simulations were started from many different initial structures with different relative orientations of the peptides. The starting conformations used for the complexes include coaxial helices (with a head-to-tail arrangement and head-to-head arrangement of the helices), side-by-side helices in both parallel and antiparallel orientations, and several misaligned arrangements of helices and globules. Simulations were performed with a variety of the basic sites protonated and the acidic sites deprotonated but the overall charge on the complex was maintained at +2 (the charge state studied in the experiments). A more detailed account of the charge distributions employed in the simulations will be given in the Results section. The MD simulations employed simulated annealing with a linear cooling schedule (240 ps at 600 K, 240 ps at 500 K, 240 ps at 400 K, and 480 ps at 300 K). Average collision cross sections were calculated using the empirically corrected exact hard spheres scattering model[34] from 50 snapshots taken from the last 35 ps of the simulations. If the structures sampled in the MD simulations match those present in the experiment, the measured and calculated cross sections are expected to agree within 2%. All cross-section calculations were performed using MOBCAL,[44] which is available from our web site.

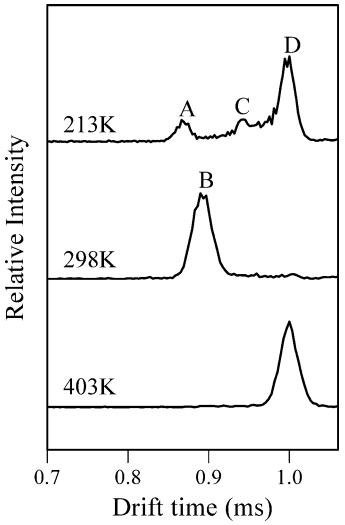

Figure 1. Drift-time distributions measured at 213, 298, and 403 K for the complex between $AcEA_7EA_7$ and AcA_7KA_6KK. The drift time scales are normalized for clarity.

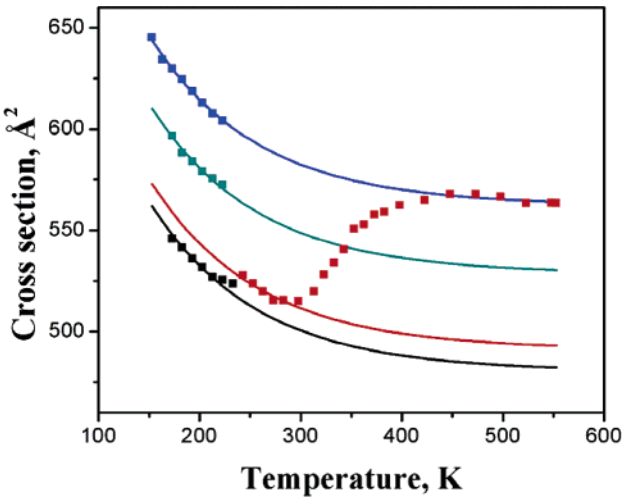

Figure 2. Plot of cross section against temperature for the complex between $AcEA_7EA_7$ and AcA_7KA_6KK. The points are the measured cross sections, and the lines correspond to fits with the exponential function described in the text. Peak **A** is shown in black, peak **B** in red, peak **C** in green, and peak **D** in blue.

Results

Room-temperature drift-time distributions measured for the uncomplexed singly charged E and K peptides both have two peaks, corresponding to a helix and globule (a random-looking, compact, three-dimensional structure). The peak assigned to the helix is the major one for both peptides. Mobility measurements were performed for the $AcEA_7EA_7 \cdot AcA_7KA_6KK+2H^+$ complex as a function of temperature from 173 to 563 K in 10-K increments. Figure 1 shows the drift-time distributions measured at 213, 298, and 403 K. Three peaks are observed at low temperatures, while only a single peak persists above 250 K.

Figure 2 shows cross sections for the main features in the drift-time distributions plotted against temperature. As the

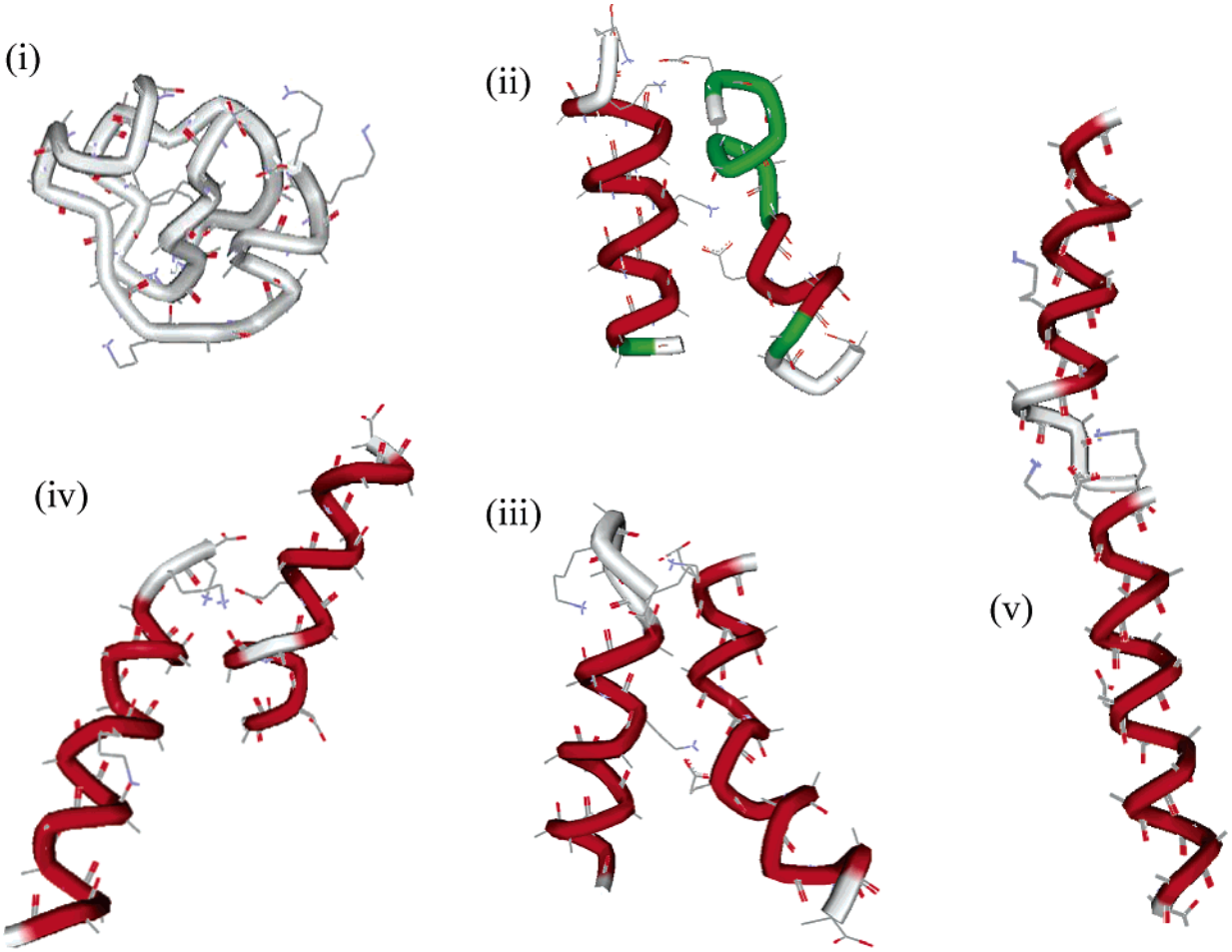

Figure 3. Representative low-energy structures from the MD simulations for the complex between $AcEA_7EA_7$ and AcA_7KA_6KK. The structures are (i) a globular complex; (ii) distorted coiled-coil; (iii) coiled-coil; (iv) misaligned coiled-coil; and (v) coaxial linear.

temperature is raised, the long-range attractive interactions between the ion and buffer gas become less important, and the cross sections systematically decrease. We have found that the temperature dependence can be fit using a simple exponential function of the form $a \exp(-T/b) + c$ where a, b, and c are adjustable parameters. The fit and extrapolated temperature dependences of the peaks are shown by the lines in Figure 2. At temperatures below 220 K, three peaks (**A**, **C**, and **D**) are observed in the drift-time distributions, indicating that three conformations, or three closely related groups of conformations, are present. As the temperature is raised, peaks **C** and **D** diminish and disappear and peak **A** shifts to a slightly larger drift time (**B** at 298 K in Figure 1). As the temperature is raised further, peak **B** shifts back to the original position of peak **D**. The extrapolated room-temperature values for the four main peaks are 501, 512, 547, and 583 $Å^2$, respectively, for **A**, **B**, **C**, and **D**.

Information about the structures of the complexes was obtained by comparing the extrapolated room-temperature cross sections to calculated cross sections for geometries obtained from MD simulations. Representative structures obtained from the simulations are shown in Figure 3. Figure 3i shows a globular complex. The calculated cross section for this conformation (442 $Å^2$) is much too small to account for any of the observed features. The extrapolated room-temperature cross section for Peak **A**, the one with the smallest drift time, is about 60 $Å^2$ larger than the calculated cross sections for the globule. This shows conclusively that the complexes all have much less compact structures than the globular conformation.

Since the helix is the main conformation observed for the uncomplexed E and K peptides, it is reasonable to consider the helix to be the building block for the complex. Simulations were performed starting from many different relative orientations of the two helices. E and K can interact as neutral residues to form hydrogen bonds, or they can undergo proton transfer and interact as an ion pair. Neutral E and K residues only interact weakly in the simulations, and they quickly become uncoupled. On the other hand, ionized E and K residues (generated by proton transfer from E to K) interact strongly and remain coupled throughout the simulation. It is not feasible to allow proton transfer to occur within the simulations, so it is necessary to start the simulations from a variety of different charge permutations. For the maximum number of strong EK interactions, the three K residues in the K peptide were protonated and the two E residues in the E peptide were deprotonated. In addition, the E peptide was protonated near the C-terminus to bring the total charge on the complex to +2. Previous studies have shown that the preferred location for a proton or a metal ion on a helix without a basic group is the backbone carbonyl groups near the C-terminus.[45] Simulations were also done with one or both of the EK pairs neutralized (weakly interacting). The overall charge on the complex was maintained at +2. At least 20 simulated annealing runs were performed for each starting structure for each charge permutation. The same basic geometries were found for the different charge permutations.

Figure 3 shows representative, low-energy structures obtained from the MD simulations. The peptides were designed with the idea that the complex should form a coiled-coil geometry. This

type of geometry is shown in parts ii and iii of Figure 3. In Figure 3ii, which we call a distorted coil-coil, one of the helices is distorted by interactions with the central E and K. In the other geometry, Figure 3iii, the helices are less distorted, but they are also less closely packed. The calculated cross section for the distorted structure in Figure 3ii (492 Å^2) is close to the extrapolated value for peak **A (**501 Å^2**).** The calculated cross section for the coiled-coil structure shown in Figure 3ii (514 Å^2) matches the extrapolated value for peak **B (**512 Å^2). The cross sections for peaks **A** and **B** are quite similar, and we are cautious about making assignments based on small differences. However, it seems clear that peaks **A** and **B** are most likely due to geometries that have two nearly side-by-side helices.

Peak **C** is a minor peak only observed at low temperatures. The fact that it disappears as the temperature is raised suggests that it may be due to a metastable geometry that can be annealed away. The extrapolated cross section for peak **C** (547 Å^2) matches the calculated cross section for the misaligned coiled-coil structure represented in Figure 3iv (552 Å^2). In the misaligned coiled-coil, the KK group on the AcA_7KA_6KK peptide interacts with the middle E residue of the $AcEA_7EA_7$ peptide. This structure is missing an EK interaction that is present in the coiled-coil and the distorted coiled-coil geometries.

The cross sections for the dominant low-temperature peak **D** appear to extrapolate to match those of the high-temperature peak, suggesting that these features share a common conformation. The cross sections for this conformation are the largest ones measured for the complex, indicating that this is due to the most open conformation. The extrapolated cross section for Peak **D (**583 Å^2) matches the calculated cross section for the coaxial linear complex shown in Figure 3v (582 Å^2). In the coaxial linear conformation, there is an interaction between the KK group in the AcA_7KA_6KK peptide and the E residue at the N-terminus of the $AcEA_7EA_7$ peptide; however, the interaction between the middle E and K residues (which is present in the geometries with side-by-side helices) is broken.

At room temperature, a single narrow peak (**B**) is observed, with a cross section that corresponds to the coiled-coil structure. As the temperature is raised, the cross section smoothly increases to a value that matches the cross section for the coaxial linear structure. So the increase in cross section between 300 and 400 K presumably corresponds to a conformational change from a coiled-coil structure to a coaxial linear arrangement. The fact that this change occurs with a narrow peak sliding smoothly from the position of the coiled-coil to the position of the coaxial linear arrangement suggests that the two conformations interconvert rapidly on the experimental time scale (if the transition occurred on a time scale comparable to the drift time, the peak would be broadened and extend from the position of the coiled-coil to the position for the coaxial linear arrangement). Since the two conformations interconvert rapidly, the position of the resulting narrow peak reflects the amount of time spent in each conformation. For example, if the complex spends most of the time in the coiled-coil arrangement, the peak will be closer to the expected position of the coiled-coil, and if it spends half its time in each configuration, the peak will be at the halfway position between the two peaks. Since the time spent in each conformation is proportional to their concentration, it is possible to extract an equilibrium constant for the transition between the two conformations from the cross section data shown in Figure 2. To do this, we need to be able to predict the temperature dependence of the cross sections in the absence of the conformational change (as shown by lines in Figure 2). The basic assumption behind this approach is that we are dealing with a two-state problem involving only the coiled-coil structure and the coaxial linear structure.

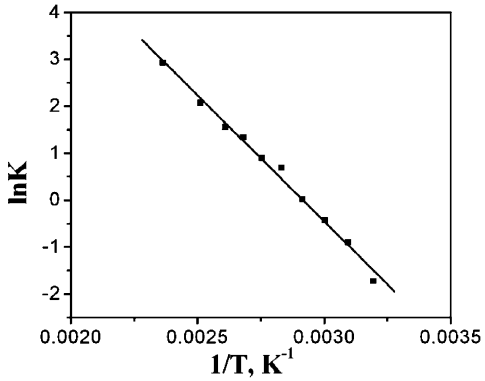

Figure 4. Plot of ln K vs 1/*T* for the complex between AcA_7KA_6KK and $AcEA_7EA_7$.

Figure 4 shows a plot of ln K against 1/*T*. The enthalpy change ($\Delta H°$) and entropy change ($\Delta S°$) for the opening of the coiled-coil to the coaxial linear structure can be obtained from the slope and intercept of the plot. $\Delta H°$ is found to be -60 ± 4 kJ mol^{-1}, and $\Delta S°$ is 193 ± 4 JK^{-1}mol^{-1}.

Discussion

The structural assignments described above are based on a comparison of the measured and calculated cross sections. This approach can unambiguously rule out some conformations. For example, the globular conformation is ruled out because the measured cross sections are all significantly larger than expected for a low-energy globule. Since the complexes are not globules, we have assumed that they are assembled from helical building blocks. This is a reasonable assumption because the constituent peptides prefer helical conformations. The helix is a stable conformation in the gas phase, and the peptides employed here were designed to be helical. The antiparallel coiled-coil geometry and the extended coaxial linear geometry are two reasonable ways of organizing the helices in the complex. The coaxial linear geometry has a large cross section, and it is unique in the sense that it is the only geometry assembled from helices that can achieve such a large cross section. The calculated geometries are derived from force-field calculations, and there remain open questions about some aspects of these calculations. So assignments of geometries based on small differences in the cross sections, such as differentiating between the distorted coiled-coil and the coiled-coil geometries, should be treated with caution.

The coiled-coil structures are stabilized by an EK and an EKK interaction and by favorable interhelical interactions, particularly those involving the helix macrodipoles. An α-helix has a large dipole moment, and in the structures shown in part ii and iii of Figure 3, the helices and their dipoles are aligned in a favorable antiparallel arrangement. In previous studies of mixed alanine/glycine peptides, an antiparallel helical dimer (linked by exchange lysines) was observed even though the monomer is predominantly in a globular conformation.[38,39] Thus the electrostatic interactions between the helix dipoles can help stabilize the helical conformation in the coiled-coil arrangement.

The presence of an E or K residue in the middle of a sequence destabilizes helices due to an unfavorable interaction of the charge with the helix dipole (if the residue is charged) and by competing with the backbone hydrogen bonds (if the residue is charged or neutral). The destabilizing effect of an E residue in unsolvated alanine/glycine-based peptides was evident in a

previous study.[46] In the present case, the destabilizing influence leads to the distorted coiled-coil geometry where one of the helices is partially disrupted.

Opening of the coiled-coil structure to the coaxial linear geometry occurs between 300 and 400 K. Values were derived for the enthalpy and entropy changes for this process from an analysis of the experimental results assuming a two-state equilibrium ($\Delta H° = -60 \pm 4$ kJ mol^{-1} and $\Delta S° = 193 \pm 4$ J K^{-1} mol^{-1}). Conversion of the coiled-coil to the coaxial linear structure presumably involves the breaking of the middle EK interaction. There are also interhelical interactions that need to be broken, including those between the helix dipoles. An estimate of the interhelical interactions can be obtained from recent studies of the $AcA_{14}KG_3A_{14}K+2H^+$ peptide in the gas phase.[47] This peptide can adopt a helix-turn-helix motif (a coiled-coil geometry with the turn at the three central glycines) and a coaxial linear conformation analogous to the two main conformations observed here. The helix-turn-helix opens up to the coaxial linear conformation as the temperature is raised (analogous to the transition reported here). Analysis of the results assuming a two-state equilibrium yielded $\Delta H° = -45 \pm 2$ kJ mol^{-1} and $\Delta S° = 114 \pm 5$ J K mol^{-1}. By assumption that the $\Delta H°$ value for the helix-turn-helix is mainly due to interhelical interactions, this suggests that the EK interaction in complex 1 contributes around 15 kJ mol^{-1} to the enthalpy change for opening up the coiled-coil. The calculated energy for a neutral hydrogen bond between an acid and an amine is 20−60 kJ mol^{-1}, and for an ion pair interaction, it is reported to be 500−580 kJ mol^{-1}.[48,49] Thus the portion of the enthalpy change for opening the coiled-coil structure attributed to the EK interaction (around 15 kJ mol^{-1}) is consistent with a neutral hydrogen bond. Note that, if an ion pair was formed, we would not expect to recover the full ion-pair interaction energy because there is an energetic cost associated with forming an ion pair from neutral residues. Ion-pair formation will only occur when the sum of the energetic cost for making the ion pair and the ion-pair interaction energy exceeds the energy of a neutral hydrogen bond. Thus ion pair formation could result in an overall EK interaction energy that is only slightly larger than for a neutral hydrogen bond. In the present case, the small value for the EK interaction clearly favors a neutral hydrogen bond. The larger entropy change for the complex (193 ± 4 J K^{-1} mol^{-1}) compared to the $AcA_{14}KG_3A_{14}K+2H^+$ peptide (114 ± 5 J K^{-1} mol^{-1}) must be at least partly due to the side chain entropies of the E and K residues that are uncoupled when the complex opens up to the coaxial linear geometry.

The coaxial linear geometry shown in Figure 3v has an EKK interaction between the KK at the C terminus of AcA_7KA_6KK and the E at the N terminus of $AcEA_7EA_7$. The EK interaction at the middle of the helices is broken. In the EKK interaction, both K residues can interact simultaneously with the E forming a + − + salt bridge. Salt bridge interactions between two Ks and an E are known to be stronger in solution than an EK ion-pair interaction.[6] However, in the gas phase, formation of salt bridges is less favorable than in solution because of the absence of solvation. Thus, the overall energy of the KEK + − + salt bridge may be similar to the energy of an arrangement where one K is protonated and the other K and the E are neutral.

The coaxial linear conformation survives to around 563 K, at which point the signal due to the complex has decreased to approximately 10% of its room temperature value due to dissociation. Thus the EKK interaction is significantly stronger than the interactions maintaining the coiled-coil geometry: the coiled-coil unfolds at 300−400 K, while the complex dissociates between 500 and 600 K. For the coiled-coil geometry, the EK interaction is thought to be a minor contributor to the overall unfolding energy (the main contribution appears to come from interhelical interactions including those due to the helix dipoles). For the coaxial linear geometry on the other hand, interhelical interactions are not expected to be a significant contributor to the overall stability. The helix dipoles do not interact favorably, and the contact area between the two helices is small so there is not a substantial van der Waals contribution. Thus the EKK interaction is expected to be the major contributor to the dissociation energy of the complex, and so the EKK interaction must be substantially larger than the EK interaction.

The nature of the interaction between E and K may depend on the positions of the residues. It has been shown that the pK_a value of a charged residue is dependent on its position within a helix.[50,51] For example, the pK_a of an E residue at the N-terminus of a helix is lower than at the middle or at the C-terminus.[50] This is due to the interaction of the charge with the helix macrodipole. Hence, ionization of a lysine at the C-terminus of the K peptide and of a glutamic acid at the N-terminus of the E peptide is expected to be more favorable than ionization of these residues in the center of a helix. Furthermore, since one of the K residues in the EKK group at the termini of the helices is expected to be ionized, there is the possibility that the charge will also promote ion-pair formation in the nearby E and K residues to form a + − + salt bridge.[52,53] This would account for the much greater strength of the EKK interaction at the termini of the helices compared to the EK interaction at the middle.

Conclusions

The complex studied here was designed to adopt an antiparallel coiled-coil geometry with an EK interaction in the middle and an EKK interaction at one of the ends. The coiled coil geometry unfolds between 300 and 400 K to a coaxial linear geometry. This transition involves the breaking of the middle EK interaction. By assumption of a two-state equilibrium, the enthalpy for unfolding was found to be 60 ± 4 kJ mol^{-1}, most of which is attributed to interhelical interactions. The small EK interaction deduced here (around 15 kJ mol^{-1}) is consistent with a neutral hydrogen bond. On the other hand, the EKK interaction, which is responsible for tethering the helices together in the coaxial linear geometry, appears to be much stronger than the middle EK interaction, because the complex survives to between 500 and 600 K. The EKK interaction may be a salt bridge stabilized by a charged lysine and by the helix macrodipoles.

Acknowledgment. We gratefully acknowledge the support of this work by the National Institutes of Health. We thank Jiri Kolafa for the use of his MACSIMUS programs.

References and Notes

(1) Sali, D.; Bycroft, M.; Fersht, A. R. *J. Mol. Biol.* **1991**, *220*, 779−788.

(2) Scholtz, J. M.; Qian, H.; Robbins, V. H.; Baldwin, R. L. *Biochemistry* **1993**, *32*, 9668−9676.

(3) Lumb, K. J.; Kim, P. S. *Science* **1995**, *268*, 436−439.

(4) Waldburger, C. D.; Schildbach, J. F.; Sauer, R. T. *Nat. Struct. Biol.* **1995**, *2*, 122−128.

(5) Wimley, W. C.; Gawrisch, K.; Creamer, T. P.; White, S. H. *Proc. Natl. Acad. Sci. U.S.A.* **1996**, *93*, 2985−2990.

(6) Olson, C. A.; Spek, E. J.; Shi, Z.; Vologodskii, A.; Kallenbach, N. R. *Proteins: Struct., Funct., Genet.* **2001**, 44, 123−132.

(7) Makhatadze, G. I.; Loladze, V. V.; Ermolenko, D. N.; Chen, X.; Thomas, S. T. *J. Mol. Biol.* **2003**, *327*, 1135−1148.

(8) Bosshard, H. R.; Marti, D. N.; Jelesarov, I. *J. Mol. Recognit.* **2004**, *17*, 1−16.
(9) Marqusee, S.; Baldwin, R. L. *Proc. Natl. Acad. Sci. U.S.A.* **1987**, *84*, 8898−8902.
(10) Lyu, P. C.; Gans, P. J.; Kallenbach, N. R. *J. Mol. Biol.* **1992**, *223*, 343−350.
(11) Scholtz, J. M.; Qian, H.; Robbins, V. H. Baldwin, R. L. *Biochemistry* **1993**, *32*, 9668−9676.
(12) Huyghues-Despointes, B. M. P.; Baldwin, R. L. *Biochemistry* **1997**, *36*, 1965−1970.
(13) Shi, Z.; Olson, C. A.; Bell, A. J., Jr.; Kallenbach, N. R. *Biopolymers* **2001**, *60*, 366−380.
(14) Litowski, J. R.; Hodges, R. S. *J. Biol. Chem.* **2002**, *277*, 37272−37279.
(15) Suckau, D.; Shi, Y.; Beu, S. C.; Senko, M. W.; Quinn, J. P.; Wampler, F. M.; McLafferty, F. W. *Proc. Natl. Acad. Sci. U.S.A.* **1993**, *90*, 790−793.
(16) Gross, D. S.; Schnier, P. D.; Rodriguez-Cruz, S. E.; Fagerquist, C. K.; Williams, E. R. *Proc. Natl. Acad. Sci. U.S.A.* **1996** *93*, 3143−3148.
(17) Kaltashov, I. A.; Fenselau, C. *Proteins: Struct., Funct., Genet.* **1997**, *27*, 165−170.
(18) Valentine, S. J.; Clemmer, D. E. *J. Am. Chem. Soc.* **1997**, *119*, 3558−3566.
(19) Wyttenbach, T.; Bushnell, J. E.; Bowers, M. T. *J. Am. Chem. Soc.* **1998**, *120*, 5098−5103.
(20) Schaaff, T. G.; Stephenson, J. L.; McLuckey, S. L. *J. Am. Chem. Soc.* **1999**, *121*, 8907−8919.
(21) Jarrold, M. F. *Annu. Rev. Phys. Chem.* **2000**, *51*, 179−207.
(22) Ruotolo, B. T.; Verbeck, G. F.; Thomson, L. M.; Gillig, K. J.; Russell, D. H. *J. Am. Chem. Soc.* **2002**, *124*, 4214−4215.
(23) Light-Wahl, K. J.; Schwartz, B. L.; Smith, R. D. *J. Am. Chem. Soc.* **1994**, *116*, 5271−5278.
(24) Loo, J. *Int. J. Mass Spectrom.* **2000**, *200*, 175−186.
(25) Smith, R. D. *Int. J. Mass Spectrom.* **2000**, *200*, 509−544.
(26) Daniel, J. M.; Friess, S. D.; Rajagopalan, S.; Wendt, S.; Zenobi, R. *Int. J. Mass Spectrom.* **2002**, *216*, 1−27.
(27) Counterman, A. E.; Valentine, S. J.; Srebalus, C. A.; Henderson, S. C.; Hoagland, C. S.; Clemmer, D. E. *J. Am. Soc. Mass Spectrom.* **1998**, *9*, 746−759.
(28) Lee, S.-W.; Beauchamp, J. L. *J. Am. Soc. Mass Spectrom.* **1999**, *10*, 347−351.
(29) Hudgins, R. R.; Jarrold, M. F. *J. Am. Chem. Soc.* **1999**, *121*, 3494−3501.
(30) Hagen, D. F. *Anal. Chem.* **1979**, *51*, 870−874.
(31) Von Helden, G.; Hsu, M. T.; Kemper, P. R.; Bowers, M. T. *J. Chem. Phys.* **1991**, *95*, 3835−3837.
(32) Clemmer, D. E.; Jarrold, M. F. *J. Mass Spectrom.* **1997**, *32*, 577−592.
(33) Hudgins, R. R.; Ratner, M. A.; Jarrold, M. F. *J. Am. Chem. Soc.* **1998**, *120*, 12974−12975.
(34) Hudgins, R. R.; Jarrold, M. F. *J. Phys. Chem. B* **2000**, *104*, 2154−2158.
(35) Hartings, M. R.; Kinnear, B. S.; Jarrold, M. F. *J. Am. Chem. Soc.* **2003**, *125*, 3941−3947.
(36) Counterman, A. E.; Clemmer, D. E. *J. Am. Chem. Soc.* **2001**, *123*, 1490−1498.
(37) Kaleta, D. T.; Jarrold, M. F**.** *J. Am. Chem. Soc.* **2002**, *124*, 1154−1155.
(38) Kaleta, D. T.; Jarrold, M. F. *J. Phys. Chem. A* **2002**, *106*, 9655−9664.
(39) Kaleta, D. T.; Jarrold, M. F. *J. Phys. Chem. B* **2003**, *107*, 14529−14536.
(40) Kohtani, M.; Jones, T. C.; Schneider, J. E.; Jarrold, M. F. *J. Am. Chem. Soc.* **2004** *126*, 7420−7421.
(41) Kinnear, B. S.; Hartings, M. R.; Jarrold, M. F. *J. Am. Chem. Soc.* **2001**, *123*, 5660−5667.
(42) Mason, E. A.; McDaniel, E. W. *Transport Properties of Ions in Gases*; Wiley: New York, 1988.
(43) Kolafa, J. http://www.icpf.cas.cz/jiri/macsimus/default.htm.
(44) Mesleh, M. F.; Hunter, J. M.; Shvartsburg, A. A.; Schatz, G. C.; Jarrold, M. F. *J. Phys. Chem.* **1996**, *100*, 16082−16086.
(45) Kohtani, M.; Kinnear, B. S.; Jarrold, M. F. *J. Am. Chem. Soc.* **2000**, *122*, 12377−12378.
(46) Sudha, R.; Kohtani, M.; Breaux, G. A.; Jarrold, M. F. *J. Am. Chem. Soc.* **2004**, *126*, 2777−2784.
(47) Kaleta, D. T.; Jarrold, M. F. *J. Am. Chem. Soc.* **2003**, *125*, 7186−7187.
(48) Grabowski, S. J. *J. Phys. Org. Chem.* **2004**, *17*, 18−31.
(49) Hodoscek, M.; Hadzi, D. *J. Mol. Struct.* **1989**, *198*, 461−473.
(50) Joshi, H. V.; Meier, M. S. *J. Am. Chem. Soc.* **1996**, *118*, 12038−12044.
(51) Doig A. J.; Baldwin, R. L. *Prot. Sci.* **1995**, *4*, 1325−1336.
(52) Jockusch, R. A.; Price, W. D.; Williams, E. R. *J. Phys. Chem. A* **1999**, *103*, 9266−9274.
(53) Julian, R. R.; Beauchamp, J. L.; Goddard, W. A. *J. Phys. Chem. A* **2002**, *106*, 32−34.